Joint Damping and Nonlinearity in Dynamics of Space Structures

Mary Bowden* and John Dugundji†
Massachussets Institute of Technology, Cambridge, Massachusetts

The presence of joints can strongly affect the dynamics of space structures in weightlessness, especially if the joints are numerous, of low stiffness, or nonlinear. Analysis of the effect of linear joint characteristics on the vibration of a free-free, three-joint beam model shows that increasing joint damping increases resonant frequencies and increases modal damping, but only to the point at which the joint gets "locked up" by damping. This behavior is different from that predicted by modeling joint damping as proportional damping. The maximum amount of passive modal damping obtainable from the joints is greater for low-stiffness joints and for modal vibrations where large numbers of joints are actively participating. A joint participation factor is defined to study this phenomenon. Analysis of the nonlinear three-joint model, with cubic springs at the joints, shows classical single-degree-of-freedom nonlinear response behavior at each resonance of the multiple-degree-of-freedom: nondoubling of response for a doubling of forcing amplitude, multiple solutions, jump behavior, and resonant frequency shifts. These properties can be concisely quantified by characteristics backbone curves, which show the locus of resonant peaks for increasing forcing amplitude. Modal coupling due to joint nonlinearity is also exhibited. Nonlinear effects are emphasized, as damping effects were, when joint activity is high, such as for low-stiffness joints, for high-amplitude vibrations, and for modes with a high joint pariticipation factor.

Nomenclature

A	= total amplitude $=\sqrt{a^2+b^2}$
a_J, b_J	= amplitudes of joint
$\boldsymbol{a}$, $\boldsymbol{b}$	= amplitude vectors
$\boldsymbol{C}$	= damping matrix
C_L	= linear joint damping
c_p, c_q	= describing function coefficients
D	= nondimensional damping factor
EI	= beam stiffness
F	= force
F_J	= joint force
F_{NL}	= nonlinear joint force
F_0	= force amplitude
JPF	= joint participation factor
$\boldsymbol{K}$	= stiffness matrix
$\boldsymbol{K}_e$	= element stiffness matrix
K_{CS}	= nonlinear cubic spring stiffness
K_J	= joint stiffness
K_L	= linear joint stiffness
$\boldsymbol{K}_T$	= total stiffness matrix
L	= joint-to-joint beam length
L_e	= finite-element length
$\boldsymbol{M}$, $\boldsymbol{M}_e$, $\boldsymbol{M}_T$	= mass, element mass, total beam mass matrices, respectively
m	= beam mass per unit length
N	= number of joints in system
q, $\dot{q}$	= generic degree of freedom and its time derivative
$\boldsymbol{q}$, $\dot{\boldsymbol{q}}$, $\ddot{\boldsymbol{q}}$	= vector of degrees of freedom and derivatives
q_J, $\dot{q}_J$	= nonlinear joint degree of freedom and derivative
t	= time
ζ	= damping ratio
λ	= ratio of element to beam length (L_e/L)
ϕ	= generic angle $= \omega t$
ω	= natural or forcing frequency
ω_0	= reference frequency

Superscript

~	= nondimensional quanitity

Introduction

ALL large truss structures designed for construction in space include complex joints to allow for on-orbit deployment or assembly. This paper investigates the effects of joint characteristics on the overall dynamics of the structure, with the goal of determining the circumstances under which a structure becomes "joint-dominated" rather than being simply a perturbation of a linear continuous system. Two key questions that arise relate particularly to the effect of joint damping and joint nonlinearity: specifically, how much passive damping can be introduced into the system via linear viscous damping in the joints, and how nonlinear will the overall truss dynamics be as a result of local joint nonlinearities? Both joint damping and joint nonlinearity should be well understood and quantified in order to design the structure to meet mission requirements and to implement effective control strategies.

Linear models of truss structures generally represent the structural joints as finite-element nodes, which are either pinned connections between bar elements (only tension and compression allowed in the elements) or clamped connections between beam elements (bending allowed also).[1] A slightly more sophisticated model would represent the joints as flexible connections with linear stiffness. If linear damping is also added at the joints, the result is a linear system with nonproportional damping, which can be treated either using time-varying normal modes[2] or complex modes. Lee[3] and Crawley and O'Donnell[4] used models with stiffness and damping in the joints to initiate the study of how linear joint characteristics

Presented as Paper 88-2480 at the AIAA SDM Issues of the International Space Station Conference, Williamsburg, VA, April 21-22, 1988; received May 19, 1988; revision received Jan. 7, 1989.

*Research Assistant, Space Systems Laboratory, Department of Aeronautics and Astronautics. Student Member AIAA.

†Professor, Department of Aeronautics and Astronautics. Member AIAA.

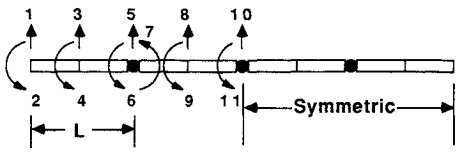

Fig. 1 Three-joint model.

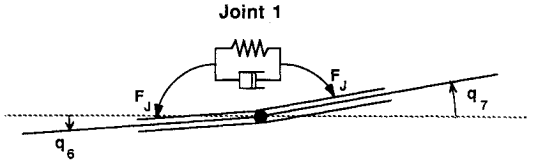

Fig. 2 Joint forces.

affect the overall dynamics of the system. The work presented in this paper is a direct continuation of that effort.

Experimental characterization of individual joints was pursued by Crawley and Aubert[5] and by Belvin,[6] who developed a force-state mapping technique to measure the parameters of a joint. To enhance the inherent passive damping in structures, a number of joints were designed and built by Prucz et al.,[7,8] using viscoelastic materials, to show that significant damping can be obtained without unacceptable stiffness penalties. In addition, scale models of trusses with realistic joints were studied both analytically and experimentally by Hertz and Crawley[9] and by Sigler.[10]

Many standard techniques exist for modeling nonlinear systems. Classical single-degree-of-freedom (DOF) forced response is presented in many textbooks,[11,12] and Nayfeh and Mook[13] include a similar treatment for multi-DOF nonlinear systems. The harmonic balance technique has been applied with success to linearize single-DOF systems, for example, to study control surface flutter with nonlinearities.[14,15] More generally, describing functions can be used to quasilinearize any describable nonlinearity under a wide variety of excitation conditions.[16] Mercadal,[17] for example, used a describing function representation of joint free play to investigate limit cycle instabilities in the control of a long, deployable mast.

Transient response of nonlinear systems has also been treated by many researchers. Foelsche, Griffin, and Bielak[18] studied the transient response of 1- and 2-DOF nonlinear systems, also using a describing function formulation, and demonstrated good comparison with explicit time integration. Belvin[6] developed a nonlinear finite-element model for transient analysis of space structures with nonlinear joints, and Ludwigsen[19] investigated the effect of various forms of nonlinearity (geometric, buckling, and joint free play) on truss response dynamics. A very detailed model of a nonlinear sleeve joint with dry friction and impact damping was developed by Ferri,[20] and the transient response was numerically integrated. Some experimental investigation of the effects of nonlinear joints has been performed as well by Sarver,[21] who studied the dissipation and transfer of energy between modes in piecewise continuous structures with nonlinear joints.

This paper summarizes both linear and nonlinear anlayses of a simple three-joint beam model. The linear analysis deals primarily with the study of linear viscous damping in the joints which, by its very nature, is nonproportional and therefore couples the undamped vibration modes. The nonlinear analysis consists of calculating the forced response of the three-joint model with discrete nonlinearities located at the joints and shows how the effect of the nonlinearity is spread to all degrees of freedom of the system. Further details of this analysis can be found in Ref. 22. It is hoped that these studies provide further insight into the dynamic characteristics of jointed truss structures.

Linear Analysis

Jointed Model

The analyses and results presented here are all derived using a simple finite-element model of a jointed structure. As shown in Fig. 1, the model is a free-free system of four equal beams connected by three joints. Each beam is represented by two finite elements, with distributed mass and stiffness to allow it sufficient flexibility. Each joint is identical and has linear rotational stiffness and damping, in addition to nonlinear characteristics if desired (see Fig. 2). This system has 21 independent DOFs, although these can be reduced to 11 distinct DOFs for symmetric analyses. In addition to representing a simple jointed beam system, the results of this model can be extrapolated directly to represent a long truss beam if the beams are interpreted as truss bays with linear characteristics and the joints as bay interfaces with possibly nonlinear characteristics.

Equations of Motion

The finite-element formulation of the jointed beam model shown in Fig. 1 yields nondiagonal mass and stiffness matrices and a nonproportional damping matrix with entries representing linear viscous damping at the joints only (no material damping). The resulting linear equations of motion are

$$M\ddot{q} + C\dot{q} + Kq = F \tag{1}$$

The Appendix gives a detailed development of these equations, of the matrices M, C, and K, and of the external forcing terms F. These equations can be solved by first rewriting them in state space form,

$$\dot{x} = Ax + P \tag{2}$$

where

$$A = \begin{bmatrix} 0 & I \\ -M^{-1}K & -M^{-1}C \end{bmatrix}, \quad x = \begin{Bmatrix} q \\ \dot{q} \end{Bmatrix}, \quad P = \begin{Bmatrix} 0 \\ M^{-1}F \end{Bmatrix} \tag{3}$$

The eigenvalues of this reduced system are those of the original system, and the eigenvectors are generally all complex, indicating that nonproportional damping produces "mode shapes" that change shape during each vibration cycle. The study of these mode shapes and the corresponding eigenvalues reveals fundamental rules about how the location and properties of the joints affect the character of the overall response.

Jointed Mode Shapes

The values of the linear stiffness (K_L) and the linear damping (C_L) of the joints affect, to some extent, the mode shapes of the system. To illustrate the range of variation of the mode shapes due to joint stiffness, with zero joint damping, Fig. 3 compares the first six symmetric jointed mode shapes obtained for low joint stiffness, with the corresponding continuous beam (locked-joint) mode shapes. Note that the joint locations are indicated in each diagram by the dotted lines. The natural frequency corresponding to each case is also indicated in Fig. 3 in order to show the range of variation for each mode due to a change in joint stiffness from low ($K_L = 0.3\ EI/L$) to high ($K_L \to \infty$). The jointed mode shapes are characterized by cusps at each of the joint locations that fall near peaks; this happens for either one or all three joints in these symmetric mode shapes.

If linear damping is now introduced into the joints ($C_L \neq 0$), each mode shape shows a time variation during its vibration cycle, as illustrated in Fig. 4 for mode 11. At the beginning of the vibration cycle ($\omega t = 0$), the shape is that of the real part of

the complex eigenvector whereas, at quarter cycle time ($\omega t = \pi/4$), it is that of the imaginary part. Note that the node points are not stationary as they would be for an undamped mode shape. As damping C_L is increased, the imaginary part of the eigenvector increases to a maximum, and the time variation of the shape becomes more significant. Further increasing either joint damping or joint stiffness tends to "lock up" the joints so that the corresponding mode shapes tend toward those of a continuous beam. To understand this phenomenon more fully, it is important to look now at the variation of system eigenvalues as a function of joint stiffness and damping.

Variation of Eigenvalues

The effects of varying joint stiffness and joint damping in this linear model are illustrated by the root locus diagram presented in Fig. 5. This shows the paths described by the eigenvalues of the three-joint system as joint damping is increased from zero to infinity, for a number of different values of joint stiffness. Each path is an upward loop that starts on the imaginary axis at the corresponding locked-joint beam frequency. Lower joint stiffness results in a lower undamped natural frequency at which the loop starts and a larger loop. This illustrates a basic rule: the lower the joint stiffness, the more it can introduce its damping characteristics into the system dynamics.

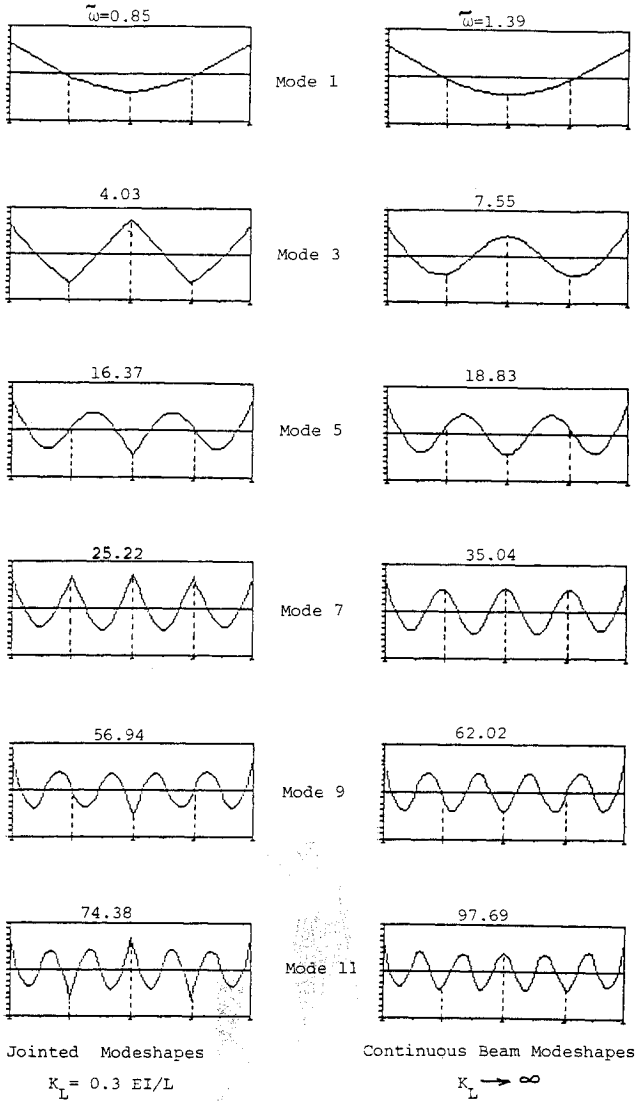

Fig. 3 Jointed and continuous beam mode shapes.

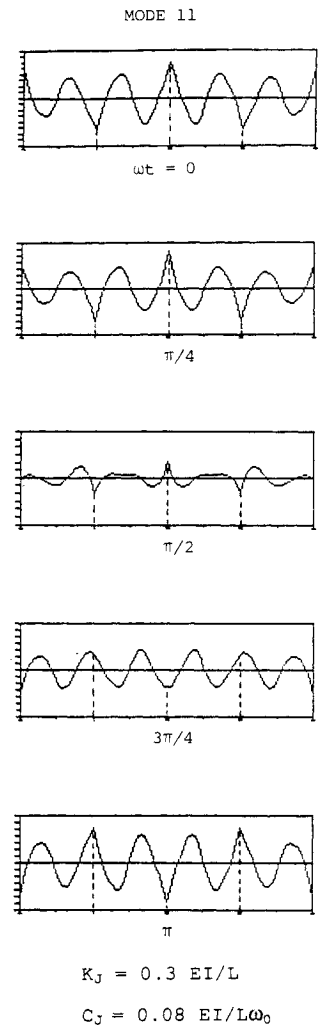

Fig. 4 Time variation of damped mode shape.

Figure 5 also shows that increasing joint damping tends to "stiffen" the structure until the joint is effectively locked by damping. More important though, increasing joint damping increases modal damping, but only to the point at which the root locus loops back. Beyond this level, the joint gets exercised less and less during modal vibration and can therefore introduce less of its damping into the system. The peak at which maximum modal damping occurs corresponds to a different value of joint damping for each mode. Another fundamental rule is apparent from this: the less a joint is exercised (whether because it is stiff or because it is vibrating in a low mode shape), the more joint damping is required to achieve maximum modal damping.

The number of joints that are active in a modal vibration also stongly affects the characteristics of that root locus. This is illustrated in Fig. 6, which presents the first six symmetric modes of the three-joint model, for a joint stiffness of $K_L = 0.3\ EI/L$. The root locus paths for these modes can be grouped into two families, as indicated by the dotted lines joining the peaks of the loops: a one-joint family (modes 1, 5, and 9 have one joint participating) and a three-joint family (modes 3, 7, and 11 have three joints participating). The three-joint family has much larger loops than the one-joint family. Similarly, a root locus diagram for the antisymmetric modes would show a zero-joint family and a two-joint family. The basic principle that results from these observations is that the greater the number of joints participating, the higher the modal damping achievable. In an attempt to make these rules more quantifiable, a joint participation factor is defined.

Joint Participation Factor

The side-by-side depiction of the jointed and continuous beam mode shapes in Fig. 3 illustrates the concept of joint participation factor (JPF), which is a geometric measure of how much the joints are exercised during a given modal vibration. The JPF is defined as follows:

$$\text{JPF} = \frac{1}{N_{\text{joints}}} \sum^{\text{all}} \left(1 - \frac{d}{\lambda/4}\right) \tag{4}$$

where

N = number of joints
d = distance of joint to nearest peak of continuous beam mode shapes
λ = wavelength of sinusoid that most closely fits mode shape (see Ref. 23).

This definition is motivated simply by realizing that the closer a joint is to a peak in the unjointed mode shape, the more it is bent in the jointed mode shape and, conversely, the closer to an inflection point (node) the less it is bent. The JPF ranges in value from 0, meaning that all joints are on nodes of the mode shape, to 1, indicating that all joints are participating to the maximum extent allowed by their stiffness. Figure 7 plots JPF vs mode number and modal damping ζ_m vs mode number, for both symmetric and antisymmetric modes. This figure indicates that whereas the JPF does increase in value when going from a zero-joint mode to a three-joint mode, it does not distinguish much between a mode with one joint participating strongly (mode 5, for example) and a mode with two joints participating only moderately (mode 6). Maximum achievable modal damping ζ_m, however, is different for the one- and two-joint modes. Thus, the JPF is only a rough indication of

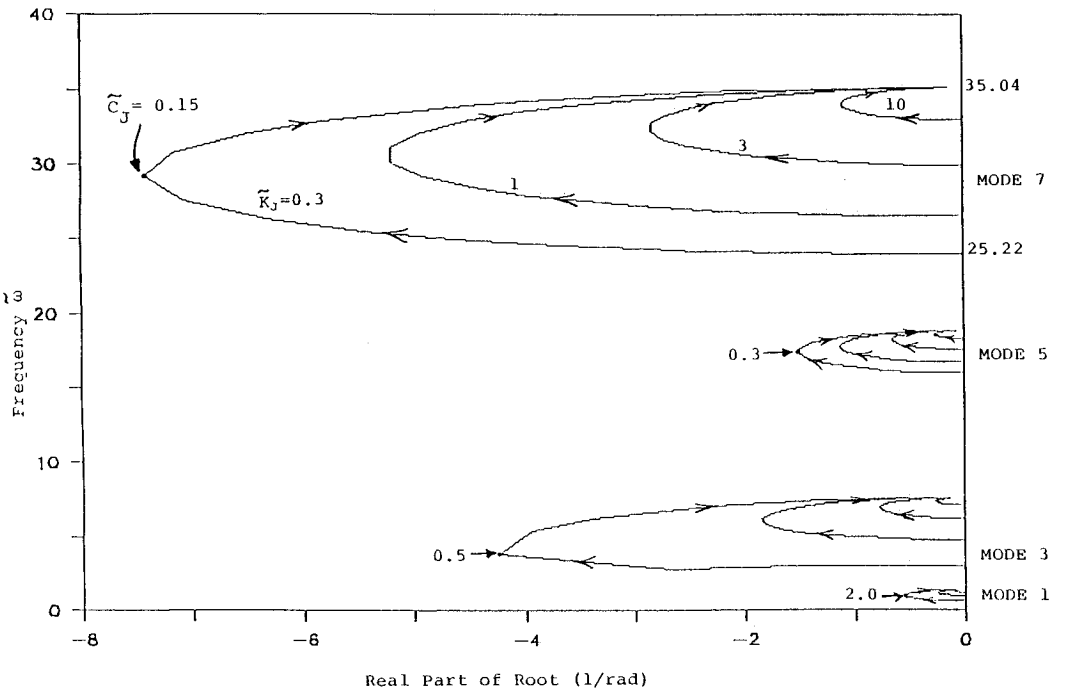

Fig 5. Root locus for varying joint stiffness.

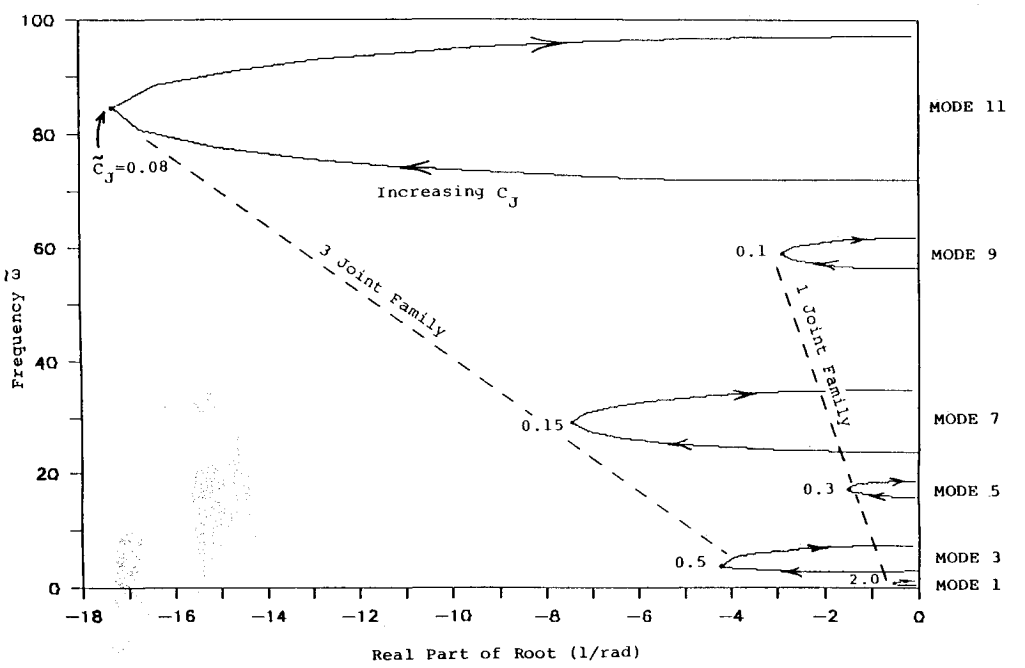

Fig. 6 Root locus for first six symmetric modes ($K_L = 0.3\ EI/L$).

how much modal damping is achievable. For more complicated models with many more joints, though, it may be a statistically significant measure of the combination of how active the joints are and how much passive damping they can provide. An alternate definition of JPF, which would represent the ratio of strain energy in the joints to strain energy in the beam, may be a more successful measure of joint participation.

Nonproportional Damping

If joint damping is known, or assumed, to be small, it is perhaps tempting to model it directly as incremental modal damping in a specific mode. This approach may be misleading because, in addition to yielding inaccurate eigenvalues, it predicts incorrect trends in the root locus behavior. To demonstrate this, the undamped eigenvectors of the three-joint system were used to transform the mass, stiffness, and damping matrices into modal form. Whereas the mass and stiffness matrices are diagonalized by this modal transformation, the nonproportional damping matrix containing joint damping terms is not diagonalized and, in fact, becomes a fully populated matrix. If only the diagonal terms of this damping matrix are kept and used to calculate damped eigenvalues, we obtain root loci, as shown in Fig. 8, that start on the imaginary axis and loop down to the real axis like a classical 1-DOF system. This path predicts that increasing joint damping lowers the resonant frequency and increases modal damping until a mode becomes overdamped. Both of these trends are incorrect for this jointed model, as is seen from the upward looping root loci described previously and shown also in Fig. 8 for comparison purposes. The correct trends due to this form of nonproportional damping can, however, be obtained from the modal model by keeping all off-diagonal terms of the transformed damping matrix when calculating eigenvalues.

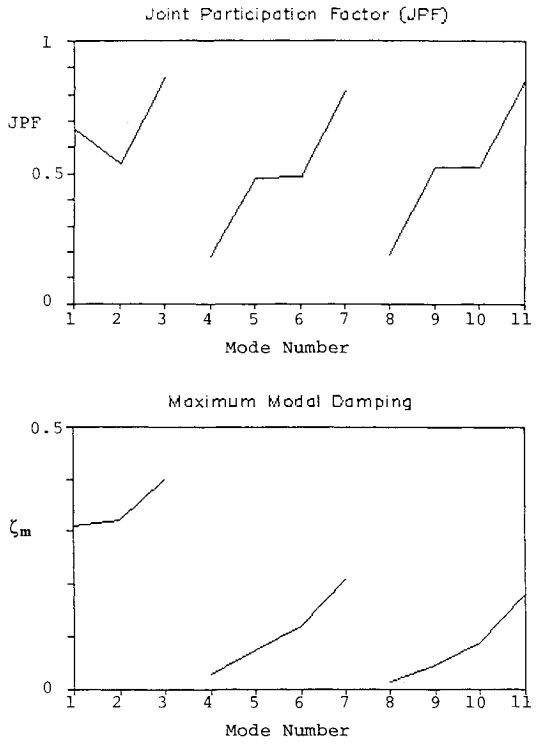

Fig. 7 JPF and ζ_m vs mode number.

Nonlinear Analysis

Describing Functions and 1-DOF Nonlinear Models

Describing functions[16] are used to introduce nonlinearities into the model of a jointed structure undergoing forced harmonic motion. It is assumed that all of the nonlinearity of the structure is localized at the joints and that all of the joints have the same nonlinear characteristics. A joint with a cubic spring is chosen to illustrate representative nonlinear behavior, but other nonlinearities (free play, coulomb friction, and combinations thereof) have also been modeled using this technique.[22] The forced harmonic response of the system is studied to determine how nonlinear the overall system dynamics are as a result of locally nonlinear joints.

The describing function formulation consists of calculating the amplitude- and frequency-dependent coefficients of the first harmonic of the nonlinear joint force. If we assume harmonic motion of the form $q = A \sin\phi$, where $\phi = \omega t$, then

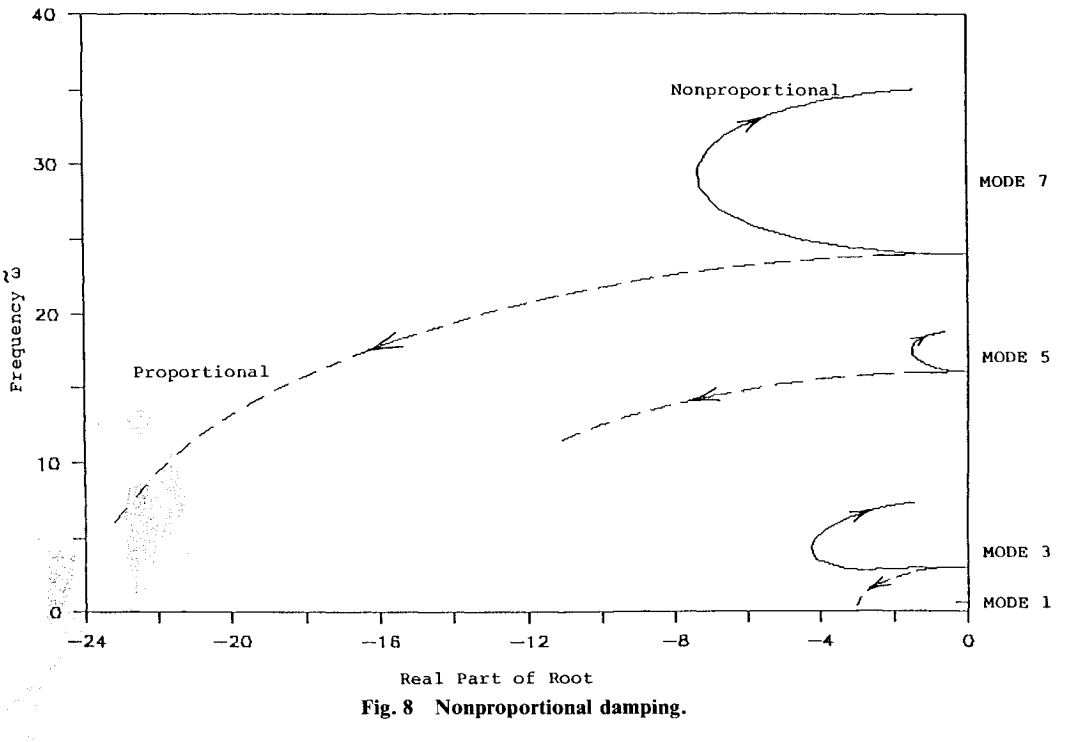

Fig. 8 Nonproportional damping.

the nonlinear force $F_{NL}(q,\dot{q})$ can be expressed as follows:

$$F_{NL} = a\sin\phi + b\cos\phi = \frac{a}{A}q + \frac{b}{A\omega}\dot{q}$$

$$= c_p q + c_q \dot{q} \tag{5}$$

where

$$c_p = \frac{1}{\pi A}\int_0^{2\pi} F_{NL}(A\sin\phi,\ A\omega\cos\phi)\sin\phi\, d\phi \tag{6}$$

$$c_q = \frac{1}{\pi A\omega}\int_0^{2\pi} F_{NL}(A\sin\phi,\ A\omega\cos\phi)\cos\phi\, d\phi \tag{7}$$

It is clear with this formulation that the nonlinearity can contribute both an additional stiffness (in-phase) term c_p and an additional damping (quadrature) term c_q that are both amplitude- and frequency-dependent. [For a nonsymmetric force F_{NL}, we would set $q = A_0 + A\sin\phi$ and include a resulting constant offset term c_0 in Eq. (5).] The full 1-DOF equation of motion for a harmonically forced nonlinear system is, thus,

$$M\ddot{q} + C_L\dot{q} + K_L q + F_{NL} = F \tag{8}$$

or replacing F_{NL} by the expression in Eq. (5),

$$M\ddot{q} + (C_L + c_q)\dot{q} + (K_L + c_p)q = F_0\sin\omega t \tag{9}$$

Assuming a solution of the form $q = a\sin\omega t + b\cos\omega t$, substituting this into Eq. (9) for q and its derivative, and balancing the sin and cos terms in this equation, we obtain a set of two equations in two unknowns, a and b. These equations are generally nonlinear because c_p and c_q are usually fairly complicated functions of a and b.

In the particular case of a 1-DOF response, this set of equations can be rearranged to give a solution for the total amplitude $A = \sqrt{a^2 + b^2}$. To obtain this expression, the original equations are nondimensionalized, squared, and added together to give

$$A^2 = \frac{(F_0/K_L)^2}{(1 - \tilde{\omega}^2 + \tilde{c}_p)^2 + \tilde{\omega}^2(2\zeta + \tilde{c}_q)^2} \tag{10}$$

where

$$\tilde{\omega} = \frac{\omega}{\omega_0}, \qquad \zeta = \frac{C_L}{2\sqrt{K_L M}} \tag{11}$$

and

$$\tilde{c}_p = \frac{c_p}{K_L}, \qquad \tilde{c}_q = \frac{c_q}{K_L}\omega_0 \tag{12}$$

This Eq. (10) can be solved iteratively to find the response amplitude A, as a function of forcing frequency ω, for any nonlinearity for which the describing function coefficients can be calculated. For a 1-DOF system, there is one resonant peak, the location of which changes as a function of forcing amplitude. To describe this variation fully, a "backbone" curve is often used to show the location of all resonant peaks. The equation for this backbone can be found by setting the system damping and the forcing equals to zero in Eq. (10) and solving for $\tilde{\omega}$:

$$\tilde{\omega}^2 = 1 + \tilde{c}_p \tag{13}$$

Because $\tilde{c}_p$ is a function of amplitude A, this represents a curve that can be plotted, along with a family of forced response curves on a graph of A vs $\tilde{\omega}$. This is shown for a nondimensional form of the cubic spring nonlinear system in Fig. 9.

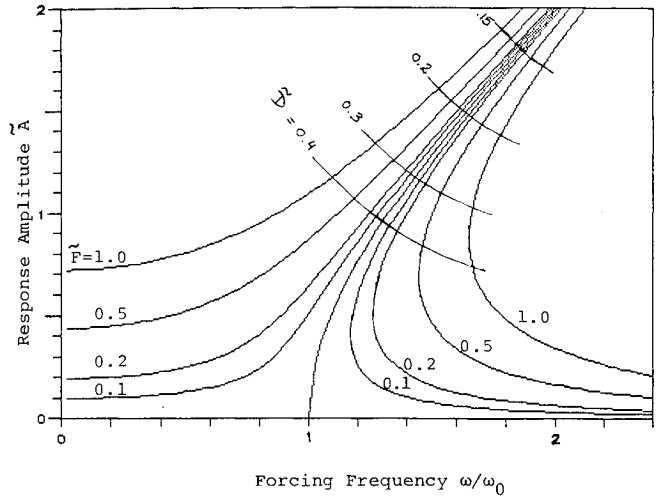

Cubic Spring Equation of Motion:

$$M\ddot{q} + C_L\dot{q} + K_L q + K_{CS}q^3 = F_0\sin\omega t$$

Define the following quantities using $\kappa = K_{CS}/K_L$

$$\tilde{q} = q\sqrt{\kappa} \qquad \tilde{A} = A\sqrt{\kappa}$$

$$\tilde{F} = \frac{F_0}{K_L}\sqrt{\kappa} \qquad \tilde{D} = \frac{\zeta}{\tilde{F}}$$

to obtain the following non-dimensional, universal form:

$$\frac{1}{\omega_0^2}\ddot{\tilde{q}} + 2\zeta\frac{1}{\omega_0}\dot{\tilde{q}} + \tilde{q} + \tilde{q}^3 = \tilde{F}\sin\omega t$$

Fig. 9 Cubic spring nonlinearity (1 DOF).

Many studies[2,11] have shown that, for a single-DOF system, nonlinear behavior can be detected by jump discontinuities in the response amplitude as the forcing frequency is varied; this corresponds to a multivaried region in the response curve. Nonlinearity is also exhibited by a nondoubling in the response amplitude as a result of a doubling of the forcing amplitude and by a shift in resonant frequency with increasing forcing amplitude.

Figure 9 illustrates these effects for the 1-DOF cubic spring joint, which generates a force

$$F_J = K_L q + K_{CS}q^3 \tag{14}$$

The describing function coefficients for this cubic spring nonlinearity are found, from Eqs. (6), (7), and (12), to be

$$\tilde{c}_p = \frac{3}{4}\frac{K_{CS}}{K_L}A^2, \qquad \tilde{c}_q = 0 \tag{15}$$

These are placed into Eq. (10) to give the results shown. Note that $A\sqrt{\kappa}$ is plotted, rather than just A, in order to normalize the asymptotic slope of the backbone curve. For a system with viscous damping as well, the response curve reaches its peak and crosses the backbone curve at the level indicated by the $\tilde{D}$ cross marks. All of these nonlinear phenomena are found to exist in multi-DOF systems with nonlinear joints, but with some interesting differences that will be illustrated in the following sections.

Multi-DOF Nonlinear Equations of Motion

The representation of nonlinear joints in the three-joint model leads to nonlinear terms in the equations of motion somewhat more complicated than for the single-DOF system

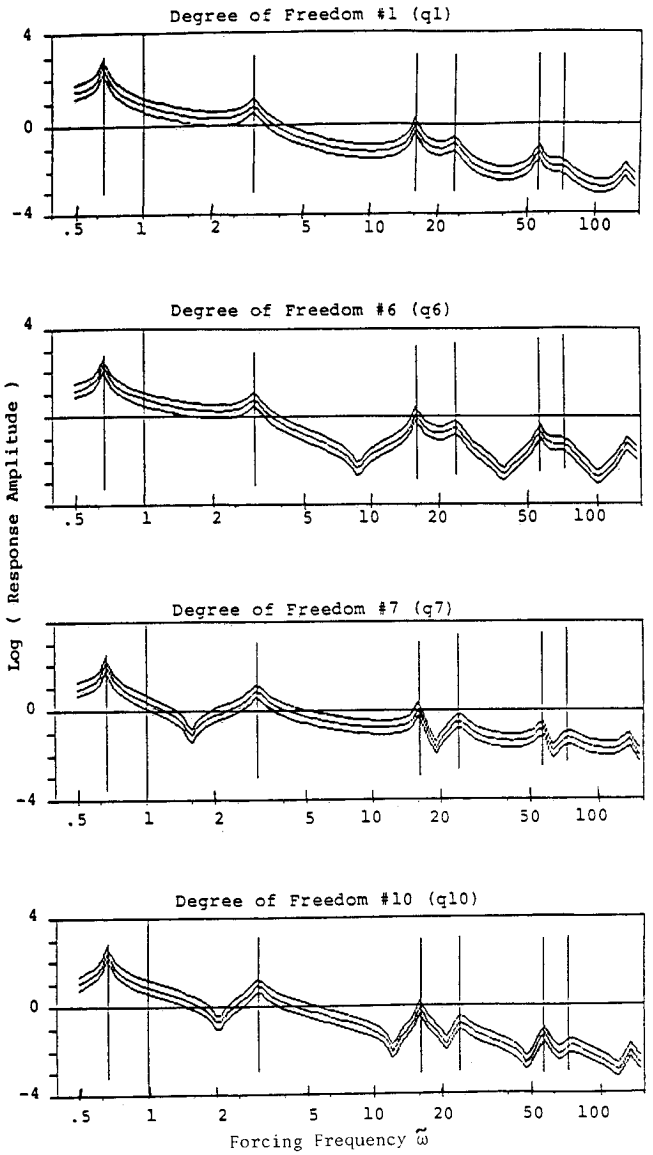

Fig. 10 Response of linear three-joint system.

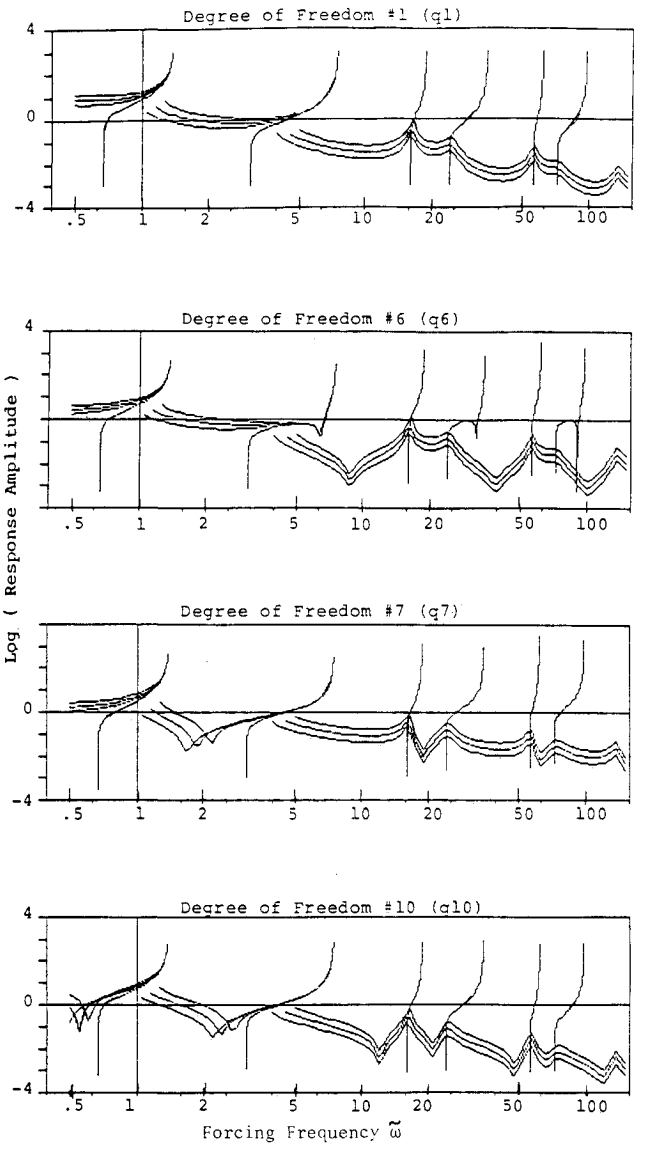

Fig. 11 Response of cubic spring system.

described previously. Each nonlinear joint contributes a nonlinear force of the form

$$F_{NL} = K_{CS} q_J^3 \tag{16}$$

where q_J represents the difference between the rotations on either side of the joint. For harmonic motion, these nonlinear terms can be represented using describing function coefficients, Eqs. (5–7), as

$$F_{NL} = c_p q_J + c_q \dot{q}_J \tag{17}$$

The describing function coefficients c_p and c_q are identical to those presented previously, except that now they are functions of the nonlinear joint amplitude (e.g., $q_J = q_7 - q_6$ for joint 1). Thus, if

$$q_J = a_J \sin\omega t + b_J \cos\omega t, \qquad A_J = \sqrt{a_J^2 + b_J^2} \tag{18}$$

the nonlinear force term becomes

$$F_{NL} = (a_J c_p - b_J \omega c_q) \sin\omega t + (a_J \omega c_q + b_J c_p) \cos\omega t \tag{19}$$

This force is added to the equations of motion for the appropriate degrees of freedom using the principle of action-reaction (see Fig. 2).

In order to write the full set of nonlinear equations of motion for the multiple-DOF system, it is convenient to formulate the assumed solution as a vector:

$$\boldsymbol{q} = \boldsymbol{a} \sin\omega t + \boldsymbol{b} \cos\omega t \tag{20}$$

so that the equations of motion become

$$\boldsymbol{M}\ddot{\boldsymbol{q}} + \boldsymbol{C}\dot{\boldsymbol{q}} + \boldsymbol{K}\boldsymbol{q} + \boldsymbol{F}_{NL} = \boldsymbol{F} \tag{21}$$

Substituting q and its derivatives into Eq. (21), and separating the sin and cos terms that result, yields a set of 22 coupled nonlinear equations in the case of the 11-DOF, three-joint model (see Appendix). A Newton-Raphson iteration technique is used to find solutions to this set of equations as a function of the forcing frequency ω. Careful selection of initial conditions for the iteration and use of a relaxation approach to aid convergence when necessary yields full response curves for all nonlinearities considered.[22] Response curves for a linear system are shown in Fig. 10, and those for a system with cubic springs at each joint are shown in Fig. 11.

A backbone curve can be defined for multi-DOF response in the same manner as for single-DOF response. As before, the backbone curve represents the locus of resonant peaks for increasing forcing amplitude, but here there is a backbone curve for each resonance of the system. Backbone curves are

computed starting with the same basic equations of motion as those shown in Eq. (21), but damping C and forcing F are set equal to zero. Given a value of response amplitude, a_1, for example, these equations are used to find a set of corresponding response amplitudes for the other degrees of freedom, a_2–a_n, and a consistent value of forcing frequency, using a Newton-Raphson iteration. Note that all of the b_i terms here are zero since $C = 0$. Backbone curves were computed for the first six resonances of the three-joint model, as shown in Figs. 10 and 11. The backbone curves in Fig. 10 are straight vertical lines at each resonance, indicating linear behavior as expected.

Nonlinear Forced Response

Figures 10 and 11 show log-log plots of the forced response of four of the degrees of freedom q_i in the three-joint model. The forcing input is a harmonic translational force applied to the central joint (DOF 10). The response amplitude is plotted as a function of the forcing frequency, for three different forcing levels ($\tilde{F}_0 = 1, 2, 4$), each representing a doubling in forcing amplitude. Figure 10 shows the linear response of the system; Fig. 11 shows the cubic spring response. As one would expect, each DOF exhibits resonant behavior at each of the natural frequencies of the system. In addition, in the nonlinear case, the response curves can jump from high-amplitude to low-amplitude response for increasing forcing frequency just as in a single-DOF system. Note that whereas a cubic spring is located only at the sixth, seventh, and eleventh DOFs of this system, when a jump occurs at any one of these locations, it happens simultaneously at all of the DOFs simply by geometric compatibility.

If the response amplitude gets large enough at any point in the response curve, it exhibits nonlinear behavior as determined by the backbone curves superimposed at each resonance. A backbone curve marks the centerline of each frequency shift which, for the cubic spring nonlinearity, goes from the jointed natural frequency of the linear system at low amplitude to the continuous beam natural frequency at high amplitude. This is, in fact, a general rule for backbone curves: they are bounded by the natural frequencies of the linear systems attained in the limit of the nonlinear behavior of the joints.

The shape of the backbone curve is a fundamental measure of how nonlinear the system response is. In addition to showing the frequency shift at a resonance, it also indicates the possible range of multivalued response. It is interesting to note that the shape of these backbone curves is very closely related to the concept of joint participation factor defined earlier using linear analysis. Thus, for example, the frequency shift for the third, seventh, and eleventh modes (three-joint modes) is much stronger than for the first, fifth, and ninth modes (one-joint modes), corresponding directly to the number of joints participating in each mode. Clearly, just as for joint damping, the more the joints participte in the modal vibration, the more their nonlinear characteristics are introduced into the system response dynamics.

Modal Coupling due to Joint Nonlinearity

It is often convenient to begin the analysis of a system with a linear model that can be reduced to a limited set of modes

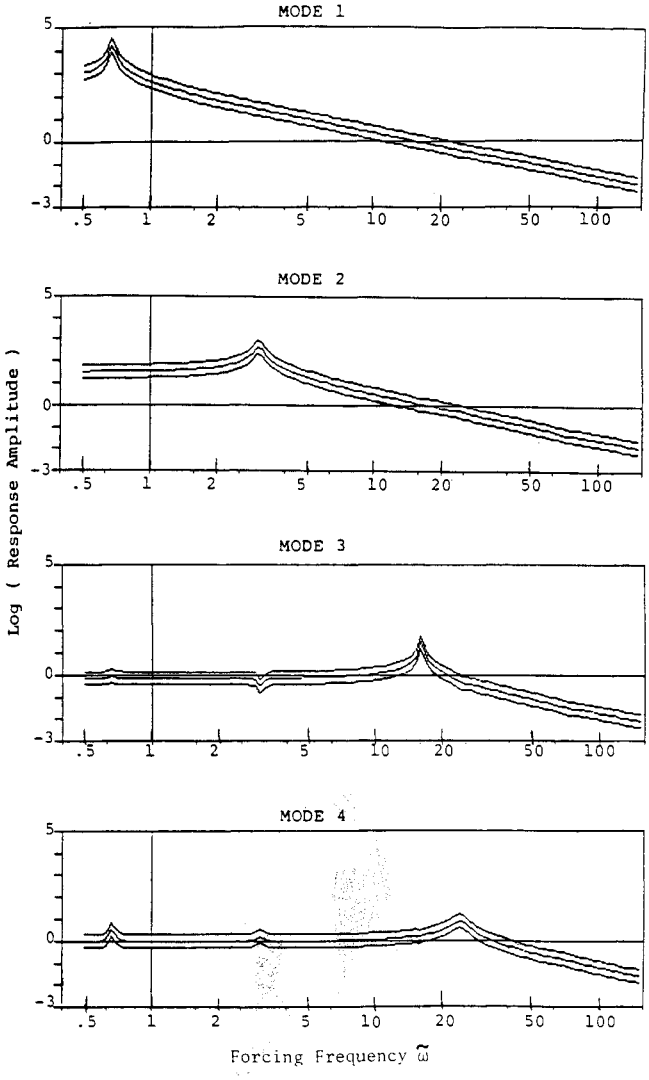

Fig. 12 Modal response of linear system.

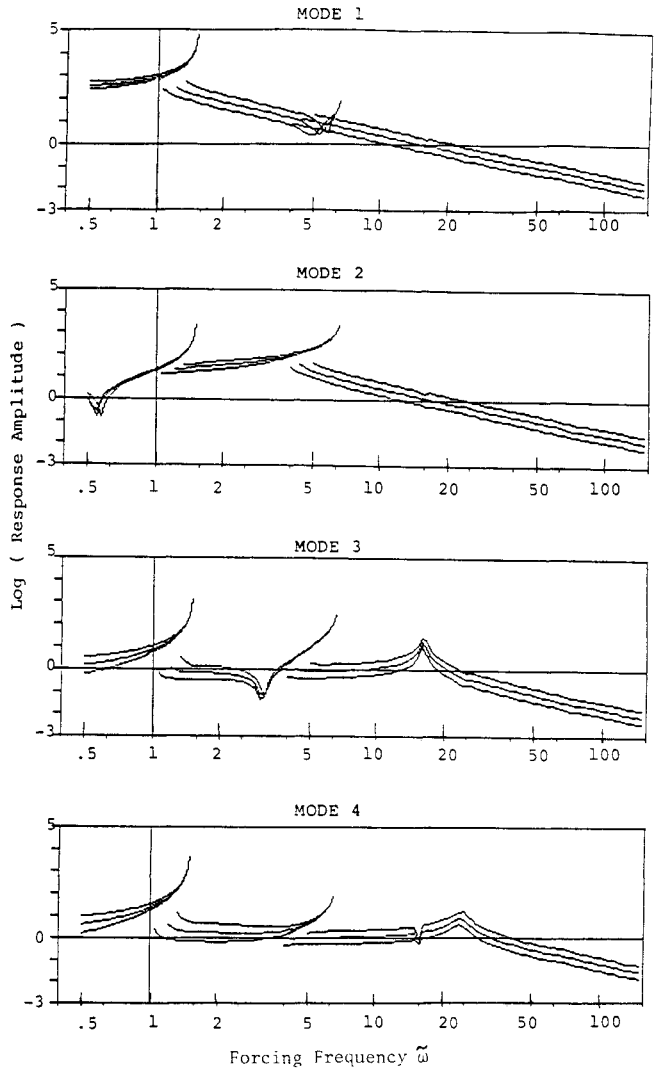

Fig. 13 Modal response of nonlinear system.

representing all of the dynamics of interest. If the system contains nonlinear joints, it is tempting to include these joints as a "perturbation" of the linear system and to continue to use the modal formulation. However, there may be modal coupling due to joint nonlinearity, in addition to the modal coupling due to nonproportional damping of the joints mentioned earlier. To illustrate the modal coupling of a nonlinear jointed system, the response of the first ten linear undamped symmetric modes of the three-joint model is calculated.

Figure 12 shows the linear response of the first four symmetric modes; Fig. 13 shows the response with joint nonlinearity included. Linear viscous damping in the joints is equal in both cases ($C_L = 0.01\ EI/L\omega_0$). In Fig. 12, each mode peaks only at its own natural frequency, except for a few perturbations due to nonproportional damping in the joints. In Fig. 13, coupling is very clear between all the modes around the first two resonant frequencies. Coupling occurs, as one would expect, whenever the response amplitude of the DOF is above the knee in the backbone curve, because this is the range in which the nonlinearity is active (see Fig. 11). Above the second resonant frequency, the response remains in the linear range of the backbone curve, and there is consequently little coupling.

Conclusions

Both the linear and nonlinear analyses presented in this paper provide insight into the global dynamics of jointed structures. The linear analyses are particularly useful in determining how damping mechanisms located in the joints distribute their effect to provide modal damping, especially to those modes that exercise the joints most actively. This concept can be quantified to some extent by the definition of a geometric joint participation factor (JPF). It is also possible to determine the level of joint damping that introduces a maximum amount of global damping into the system for any given mode. This information can be applied directly to the design of structures and joints or to the subsequent design of control systems for which the passive damping must be known. It is important to realize that, with the form of nonproportional damping present in this jointed beam model, increasing joint damping does not lower resonant frequencies or overdamp modes as increasing modal damping in a single mode would do.

The nonlinear anlayses described in this paper establish some basic rules of multi-DOF nonlinear response by illustrating how multiple discrete nonlinearities affect the global dynamics of a jointed beam system. The concept of backbone curves is presented, showing the interesting relationship between linear properties of the system, such as resonant frequencies and joint participation, and nonlinear system properties, such as the shape of the backbone curves. This paper attempts to quantify nonlinear resonant frequency shifts and response amplitudes and to determine forcing frequency ranges in which abrupt response jumps can occur. Modal coupling due to joint nonlinearity, which is also a significant aspect of nonlinear response, is calculated as well, using the techniques described in this paper.

Appendix: Jointed Beam Equations

The basic bending element is representing by spring and mass matrices as

$$K_e = \frac{EI}{L^3}\begin{bmatrix} 12/\lambda^3 & 6L/\lambda^2 & -12/\lambda^3 & 6L/\lambda^2 \\ 6L/\lambda^2 & 4L^2/\lambda & -6L/\lambda^2 & 2L^2/\lambda \\ -12/\lambda^3 & -6L/\lambda^2 & 12/\lambda^3 & -6L/\lambda^2 \\ 6L/\lambda^2 & 2L^2/\lambda & -6L/\lambda^2 & 4L^2/\lambda \end{bmatrix} \tag{A1}$$

$$M_e = \frac{mL}{420}\begin{bmatrix} 156\lambda & 22L\lambda^2 & 54\lambda & -13L\lambda^2 \\ 22L\lambda^2 & 4L^2\lambda^3 & 13L\lambda^2 & -3L^2\lambda^3 \\ 54\lambda & 13L\lambda^2 & 156\lambda & -22L\lambda^2 \\ -13L\lambda^2 & -3L^2\lambda^3 & -22L\lambda^2 & 4L^2\lambda^3 \end{bmatrix} \tag{A2}$$

where the factor $\lambda = L_e/L$, and L_e is the element length, which in this model is half the joint-to-joint beam length L. For symmetric motions, the four beam elements on the left side of Fig. 1 can be arranged in block diagonal form to create the following total system matrices (16×16):

$$K_T = \begin{bmatrix} K_e & & & \\ & K_e & & \\ & & K_e & \\ & & & K_e \end{bmatrix}, \qquad M_T = \begin{bmatrix} M_e & & & \\ & M_e & & \\ & & M_e & \\ & & & M_e \end{bmatrix} \tag{A3}$$

The potential energy U and kinetic energy T can be expressed as

$$U = \tfrac{1}{2} q_T^T K_T q_T, \qquad T = \tfrac{1}{2}\dot{q}_T^T M_T \dot{q}_T \tag{A4}$$

where q_T represents a 16×1 vector of all beam element displacements. The q_T can be reduced to 11 global operating coordinates q (Fig. 1) through the relation

$$q_T = Lq \tag{A5}$$

Here, L is a 16×11 locating matrix of appropriately placed 1's and 0's, which effectively assembles the structure. Placing q_T [Eq. (A5)] into Eq. (A4) expresses the system potential and kinetic energy in terms of the global operating coordinates q. Then, applying Lagrange's equations results in the beam structure equations

$$M\ddot{q} + Kq = Q \tag{A6}$$

where

$$M = L^T M_T L, \qquad K = L^T K_T L \tag{A7}$$

and Q represents the generalized forces on the beam corresponding to the 11 symmetric global coordinates q.

The forces Q are considered to consist of the applied external forces to the beam plus the action-reaction internal forces in the joints F_J (see Fig. 2). Assuming an external applied force $f(t)$ acting only at the center of the beam, and a linear spring K_J, linear damper C_J, and nonlinear cubic spring K_{CS} acting at the joints, we can express the generalized forces as

$$\begin{aligned} Q_6 &= K_J(q_7 - q_6) + C_J(\dot{q}_7 - \dot{q}_6) + K_{CS}(q_7 - q_6)^3 \\ Q_7 &= -K_J(q_7 - q_6) - C_J(\dot{q}_7 - \dot{q}_6) - K_{CS}(q_7 - q_6)^3 \\ Q_{10} &= \tfrac{1}{2} f(t) \\ Q_{11} &= -K_J(2q_{11}) - C_J(2\dot{q}_{11}) - K_{CS}(2q_{11})^3 \end{aligned} \tag{A8}$$

All other generalized forces $Q_i = 0$. Placing the preceding expressions into Eqs. (A6) and transposing all joint forces to the left-hand side results in the basic equations

$$M\ddot{q} + C\dot{q} + Kq + F_{NL} = F \tag{A9}$$

where C contains only linear damping terms and K contains both beam stiffness and linear joint stiffnes terms. F_{NL} represents the nonlinear joint forces, and F consists of the external applied forces. Other types of joint nonlinearities can be accommodated by modifying the F_{NL} term only. Also, antisymmetric beam motion can be modeled by setting $q_{10} = 0$, $Q_{10} = 0$, and $Q_{11} = \frac{1}{2} m(t)$, where $m(t)$ is an external applied moment acting at the center of the beam.

To determine the response to a harmonic forcing function $f(t) = f_0 \sin\omega t$, we assume displacements of the form

$$q = a \sin\omega t + b \cos\omega t \tag{A10}$$

Placing these into Eq. (A9) and gathering $\sin\omega t$ terms and $\cos\omega t$ terms results in 22 algebraic equations to be solved for the 11 a and 11 b coordinates. When nonlinear joints are present ($F_{NL} \neq 0$), the higher harmonics ($\sin 3\omega t$, $\cos 3\omega t$, . . .) are neglected, and the resulting nonlinear equations are solved by a Newton-Raphson method. For more general nonlinearities, describing functions are used to express the joint forces as

$$F_{NL} = c_p q_J + c_q \dot{q}_J \tag{A11}$$

where, $q_J = q_7 - q_6$ is a typical joint rotation and c_p and c_q are coefficients as defined in Eqs. (6) and (7). Then, for harmonic motion,

$$q_J = a_J \sin\omega t + b_J \cos\omega t \tag{A12}$$

where $a_J = a_7 - a_6$, $b_J = b_7 - b_6$, and the nonlinear joint force F_{NL} is described by Eq. (17).

For computational purposes, it is convenient to nondimensionalize the equations of motion by introducing nondimensional time $\tilde{t} = \omega_0 t$, and nondimensional coordinates $\tilde{q}_i = q_i/L$ for $i = 1,3,5,8,10$ (translational DOF) and $\tilde{q}_i = q_i$ otherwise. Also, the $i = 1,3,5,8,10$ equations are multiplied by L. This then allows us to rewrite Eq. (A9) in nondimensional form as

$$\tilde{M}\,\mathring{\tilde{q}} + \tilde{C}\,\mathring{\tilde{q}} + \tilde{K}\tilde{q} + \tilde{F}_{NL} = \tilde{F} \tag{A13}$$

where $\mathring{q} = dq/d\tilde{t}$ and the matrices $\tilde{M}$, $\tilde{C}$, $\tilde{K}$, $\tilde{F}_{NL}$, and $\tilde{F}$ are nondimensional number arrays and where joint stiffness and joint damping appear as nondimensional parameters $\tilde{K}_J$ and $\tilde{C}_J$. The reference frequency ω_0 and additional nondimensional quantities are defined here as

$$\omega_0 = \sqrt{EI/mL^4}, \qquad \tilde{\omega} = \omega/\omega_0$$

$$\tilde{K}_J = K_J L/EI, \qquad \tilde{C}_J = C_J L\,\omega_0/EI$$

$$\tilde{q}_i = \frac{q_i}{L}, \qquad \tilde{F}_i = \frac{L^2}{EI} F_i \qquad \text{for } i = 1,3,5,8,10$$

$$\tilde{q}_i = q_i, \qquad \tilde{F}_i = \frac{L}{EI} M_i \qquad \text{for } i = 2,4,6,7,9,11$$

Note that the more general joint-to-joint beam length L, is used as a reference rather than the element length L_e.

Acknowledgments

This work was supported by NASA grant NAGW-21 and by contract 85614168H from McDonnell Douglas Astronautics Company.

References

[1]Winfrey, R. C., "The Finite Element Method as Applied to Mechanisms," *Finite Element Applications in Vibration Problems,* Proceedings of the ASME Design Engineering Technical Conference, American Society of Mechanical Engineers, New York, Sept. 1977, pp. 19–39.

[2]Den Hartog, J. P., *Mechanical Vibrations*, McGraw-Hill, New York, 1940.

[3]Lee, R. Y., "Assessment of Linear and Nonlinear Joint Effects on Space Truss Booms," M.S. Thesis, Dept. of Aeronautics and Astronautics, Massachussetts Institute of Technology, Cambridge, MA, June 1985.

[4]Crawley, E. F. and O'Donnell, "A Procedure for Calculating the Damping in Multi-Element Space Structures," *Acta Astronautica*, Vol. 15, Dec. 1987, pp. 987–996.

[5]Crawley, E. F. and Aubert, A. C., "Identification of Nonlinear Structural Elements by Force-State Mapping," *AIAA Journal*, Vol. 24, Jan. 1986, pp. 155–162.

[6]Belvin, K. W., "Modeling of Joints for the Dynamic Analysis of Truss Structures," M.S. Thesis, School of Engineering and Applied Science, George Washington Univ., Washington, DC, Dec. 1985.

[7]Prucz, J., Reddy, A. D., Rehfield, L. W., and Trudell, R. W., "Experimental Charaterization of Passively Damped Joints for Space Structures," *Journal of Spacecraft and Rockets*, Vol. 23, Nov.–Dec. 1986, pp. 568–575.

[8]Prucz, J., "Analysis of Design Tradeoffs for Passively Damped Structural Joints," *Journal of Spacecraft and Rockets*, Vol. 23, Nov.–Dec. 1986, pp. 576–584.

[9]Hertz, T. J. and Crawley, E. F., "Displacement Dependent Friction in Space Structural Joints," *AIAA Journal*, Vol. 23, Dec. 1985, pp. 1996–2000.

[10]Sigler, J. L., "Prediction and Measurement of Joint Damping in Scaled Model Space Structures," M.S. Thesis, Dept. of Aeronautics and Astronautics, Massachussetts Institute of Technology, Cambridge, MA, Aug. 1987.

[11]Timoshenko, S., Young, D. H., and Weaver, W., Jr., *Vibration Problems in Engineering*, Wiley, New York, 1974.

[12]Meirovitch, L., *Elements of Vibration Analysis*, McGraw-Hill, New York, 1975.

[13]Nayfeh, A. H. and Mook, D. T., *Nonlinear Oscillations*, Wiley-Interscience, New York, 1979.

[14]Woolston, D. S., Runyan, H. L., and Andrews, R. E., "An Investigation of Effects of Certain Types of Structural Nonlinearities on Wing and Control Surface Flutter," *Journal of the Aeronautical Sciences,* Vol. 24, Jan. 1957, pp. 57–63; see also Vol. 26, Jan. 1959, pp. 51–53.

[15]Brietbach, E., "Effects of Structural Non-Linearities on Aircraft Vibration and Flutter," NATO AGARD Rept. R-665, Jan. 1978.

[16] Gelb, A. and Vander Velde, W. E., *Multiple-Input Describing Functions and Nonlinear Systems Design,* McGraw-Hill, New York, 1968.

[17]Mercadal, M., "Joint Nonlinearity Effects in the Design of a Flexible Truss Stucture Control System," M.S. Thesis, Dept. of Aeronautics and Astronautics, Massachussetts Institute of Technology, Cambridge, MA, Dec. 1986.

[18]Foelsche, G. A., Griffin, J. H., and Bielak, J., "Transient Response of Joint Dominated Space Structures: A New Linearization Technique," AIAA Paper 88-2393, April 1988.

[19]Ludwigsen, J. S., "An Assessment of the Effects of Nonlinear Behavior on the Dynamic Performance of Large Orbiting Space Stuctures," Ph.D. Thesis, Dept. of Civil Engineering, Massacussetts Institute of Technology, Cambridge, MA, Sept. 1987.

[20]Ferri, A. A., "Modeling and Analysis of Nonlinear Sleeve Joints of Large Space Structures," *Journal of Spacecraft and Rockets*, Vol. 25, Sept.–Oct. 1988, pp. 354–360.

[21]Sarver, G. L., and E. F. Crawley, "Energy Transfer and Dissipation in Structures with Discrete Nonlinearities," Space Systems Lab Report 25-87, Dept. of Aeronautics and Astronautics, MIT, Cambridge, MA, November 1987.

[22]Bowden, M. L., "Dynamics of Space Structures with Nonlinear Joints," Sc.D. Thesis, Dept. of Aeronautics and Astronautics, MIT, Cambridge, MA, May 1988.

[23]Dugundji, J., "Simple Expressions for Higher Vibration Modes of Uniform Euler Beams," *AIAA Journal*, Vol. 26, Aug. 1988, pp. 1013–1014.